Abstract

The objective of this work is to develop adequate and efficient models for calculation of vertical dynamic traffic load effects on railway track infrastructures, and applications for evaluating the comparative performance of ballast and slab track designs.

The calculations are based on dynamic finite element models with direct time integration and contact algorithms between wheel and rail in order to consider the rail-car interaction. For capturing the dynamic effects is an adequate representation of irregularities of the track. The 2D spatial discretization were selected as the optimal decisions.

The results obtained include wheel-rail contact forces, forces transmitted to the bogie by primary suspension and forces transmitted to the infrastructure (sleeper or slab) by the railpads.

Keywords: Dynamic response, Wheel-rail contact, track irregularities, Finite element, Vehicle-track interaction.

1 Introduction

High-speed railway systems have been built and operated in several countries. These are considered a competitive alternative to other modes of transport for medium distances. Spain has now in operation over 1500 km of high-speed railway lines with international gauge, with ballast track except at singular locations such as tunnels. There is an increasing need for research in order to improve the safety, reliability and efficiency of track infrastructure. The mechanical characteristics of the track and the choice between ballast and slab track are matters of debate, taking into account flying of ballast, maintenance and durability features, cost, and dynamic vertical behavior of track [1]. In this work we focus on issues related to the mechanical actions on the

track structure, specifically vertical dynamic loads.

The evaluation of the dynamic response of railway track subjected to high speed train loading represents one of the main structural issues associated specifically to the structure design of high speed railway. The dynamic behavior of railway track structures induced by the traffic is influenced by the interaction between the train and the complete track structure, and also between several elements of the rolling stock. Recently, the increasing of the operating speed of trains has received a lot of attention from researchers. As for the commercial operating speed, TGV in France and Shinkansen in Japan are being operated at about 300 km/h, ICE in Germany at 280 km/h, KTX in Korea at 300 km/h, and CRH3 in People Republic Of China is due to be operated at 350 km/h.

As the operating speed of the train becomes higher and reaches 350 km/h or more, accuracy in the analysis of vehicle-track interaction becomes an important factor to be considered in the railway track design. An important number of research works on this subject have contributed to relevant technical advantces in this area. In order to simulate the vehicle-track interactive dynamics many kinds of plane models [2–8] in which the train is treated as independent body and 3D models [3, 6, 8–12] in which the train is modeled more realistcally have been presented. As the complexity of the model increases, the analyses will require larger computer resources and time. Therefore, the optimisation of modelling both the rail track and vehicles is an important issue.

In the present paper, a dynamic computational model for the vehicle and track system is formulated by means of finite element method. Two-dimensional vehicle and track models are selected as the three-dimensional dynamic effects of vehicles do not affect significantly the vertical track dynamics. Wheel to rail contact is included as a linearized Hertz model. The track profile irregularity is modeled as a stationary ergodic random processes. The focus of this work is on obtaining reliable estimates of vertical dynamic loads on track infrastructure, namely the rail and the individual rail-pad supports. For this purpose analyses of dynamic response is performed in the time domain. The amplitudes of vibration and the interaction forces between the vehicle and rail due to the random irregularity of the track vertical profile and different train speeds have been obtained and compared at several tracks and ranges of train speeds.

2 Finite Element Models

2.1 Vehicle model

Railway vehicles are complex mechanical systems with several degrees of freedom, including linear and non-linear springs and various types of dampers. During the passage of vehicles several type of forces are applied on the track structure: vertical forces, horizontal longitudinal forces and horizontal transverses forces (Fig. 1).

In order to study the vertical dynamic track, many vehicle models have been pre-

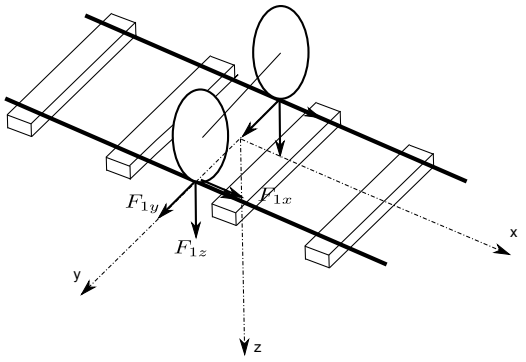

Figure 1: Forces applied to track structure: F_{1z} vertical force, F_{1x} horizontal longitudinal force, F_{1y} horizontal tranverse force.

sented in the literature: from a simple model as a moving vertical force to 3D complex model of multybody with many degrees of freedom. In this study, taking into account the 3D models are very complex, very expensive models for a computational analysis, and their frequencies outside the range of interest in frequencies for the vertical dynamic analysis, so we have developed several 2D models (see Fig. 3): one degree of freedom model (or 1/2 axle), two degrees of freedom model (1/4 bogie), and three degrees of freedom model (1/8 vehicle). The 1/2 axle model (see Fig. 3a)is a discrete mass-spring system which contains a single mass that is the mass of 1 / 2 axle-wheel m_r, the spring is presented as a Hertzian spring acting in the wheel/rail contact area k_H, and the static force acting on the mass is the weight of bogie and car $(m_b + m_c)g$. The 1/4 bogie model (see Fig. 3b) is a two-mass model, in which the other mass (mass of bogie m_b) is added over the mass in the 1/2 axle model that simulates the structure of the bogie, between the two masses is located the vehicle's primary suspension (k_1, c_1), and the static force acting on the superior mass is the weight of the car $m_c g$. The 1/8 vehicle model (see Fig. 3c) is a three-mass model, in which the other mass (mass of car m_c) is added over the masses of the 1/4 bogie model that simulates the box of the vehicle, the vehicle's secondary suspension (k_2, c_2) is located between the upper masses. In this study the data used for these models is represented in the table. 1 which represent the typical high speed vehicle with an axle load of 17 T. The results obtained with these model have been analyzed and compared in order to select the more adequate one for analyzing the relevant variables of design.

Using the Hertz theory of normal elastic contact [13] and an assumption that the wheel and the rail are elastic bodies and made of the same material with elastic modulus E and the Poisson coefficient ν. The nonlinear relationship between normal contact force F_k and relative vertical deformation δ_k is expressed

$$F_k = \delta_k^{3/2} C_H \text{ where } C_H = \frac{2E}{3(1-\nu^2)} (r_w r_r)^{1/4} \tag{1}$$

being r_w the radius wheel and r_r the radius railhead. The value of the Hertz coefficient C_H used in this study is 1.04 $N/m^{3/2}$

The 2D contact model between the wheel and the rail is mechanically presented by vertical contact stiffness k_H. The relation between the normal contact force F_k and a small deformation δ_k can be linearly represented by a linearized stiffness coefficient

Parameter	Value
1/2 Mass of wheel-axle (kg)	m_r = 758
1/2 Mass of bogie (kg)	m_b = 1395
1/8 Mass of car body (kg)	m_c = 8500
Hertz spring stiffness (KN/mm)	k_H = 1460
Primary suspension	k_1 = 0.805 kN/mm c_1 = $0.375 \cdot 10^4$ Ns/m
Second suspension	k_2 = 0.45125 kN/mm c_2 = $0.40625 \cdot 10^4$ Ns/m

Table 1: Parameters of the vehicle models per wheelset

k_H as

$$k_H = \frac{dF_k}{d\delta_k} = \frac{3}{2} F_k^{1/3} C_H^{2/3} \tag{2}$$

Then, for the solution of the contact problem in which the motion is constrained can be obtained using the penalty method.

Figure. 2 shows the comparison of dynamic response of the two models of contacts: Hertz nonlinear contact and linearized contact. The results are very similar, demonstrating the validity of linearized contact model which is used in this study.

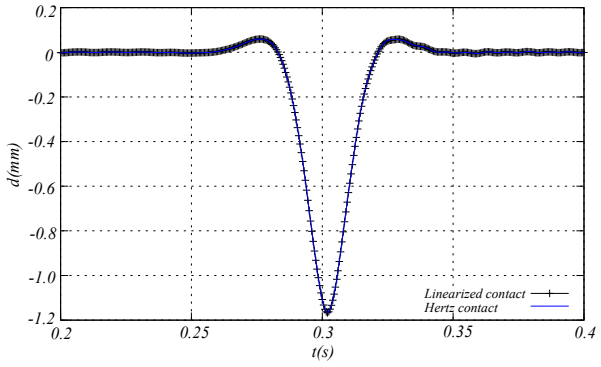

Figure 2: Deformation of the center of the rail for Hertz and linearized contact model with v=360km/h

Figure 4 shows the displacement of the rail obtained in the dynamic calculation for vehicle speed of 360 km/h with the considered models. The 1/2 axle model does not represent the reality of the passage of vehicle on the track (see fig. 3a), this model has only a single natural frequency (approx. 220 Hz) next to one of the frequencies of the Rheda track (approx. 230 Hz, see table 3) and the excitation frequency at 360 km/h with sleeper space of 0.60 m (approx. 166.66 Hz), while the real vehicle has the other relevant frequencies on the behavior of the track besides this (see table 2). Because the structural response obtained with the 1/4 bogie is very similar to the results obtained using the 1/8 vehicle model (see Fig. 4). Also, comparing the structural responses of

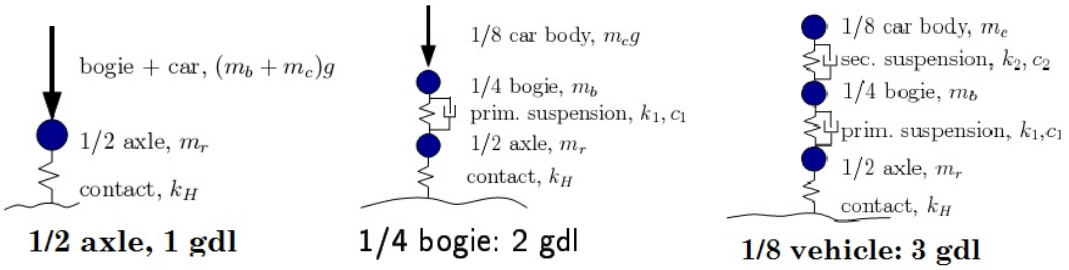

(a) One degree of freedom (b) Two degrees of freedom (c) Two degrees of freedom

Figure 3: Vehicle models

a model with a 1 / 4 bogie and model with two 1 / 4 bogie, the results are very similar (see Fig. 5), so opting for the vehicle model , the 1/4 bogie model is selected, because it's simplicity.

Model	Eigenfrequencies (Hz)
1/2 axle model	220.9 (wheelset)
1/4 bogie model	220.9 (wheelset) 3.82 (bogie)
1/8 vehicle model	220.9 (wheelset) 3.82 (bogie) 0.36 (car body)

Table 2: Eigenfrequencies of vehicle models

	Ballast	Rheda
Mode 1	110 (Hz)	- -
Mode 2	288 (Hz)	230 (Hz)
Mode 3	1200 (Hz)	1200 (Hz)

Table 3: Frequencies of relevant modes for track considered

2.2 Track model

Generally, the dynamic analysis may be carried out by models for the solution in the time-domain or models for the solution in the frequency-domain. A time-domain model of the track shown in Fig. 6 has been developed in the framework of this research [4, 5]. It fulfills the two basic requirements of linearity and periodicity with respect to the track's length direction. The finite element method was used to analyze the track system. The track system consists of the rail, the pads, the fastener, the

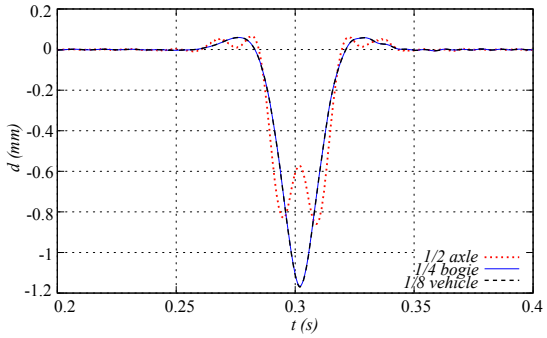

Figure 4: Deformation of the center of the rail under several vehicle models with v=360km/h

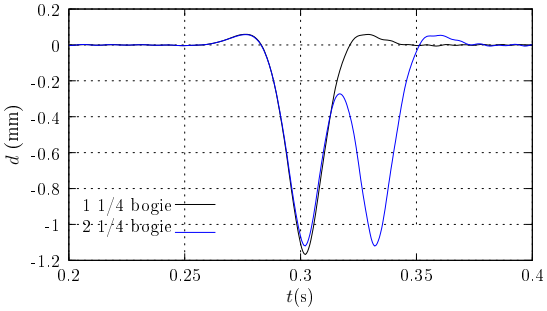

Figure 5: Deformation of center of the rail with one axle of 1/4 bogie and with two axle of 1/4 bogie with v=360km/h, for uncoupled dynamic action on track

sleeper, the ballast and the foundation in the case of ballast track model (see Fig. 6a); and the slab, the concrete bed and the foundation in the case of slab track model (see Fig. 6b).

The rails are simulated as continuous Timoshenko beams that are discretely supported on the pads and the fasteners represented by linear springs and damping elements. Each element of the rail is a two-node element with three degrees of freedom per node. Based on the Timoshenko beam theory [4], the equations (3) (4) relate the vertical deflection and the rotation at any point of the rail with the applied forces:

$$\rho A\ddot{w} - GA_s(w'' - \theta') = -\sum F(x,t) \tag{3}$$

$$\rho I\ddot{\theta} - GA_s(w' - \theta) - EIw'' = 0\,, \tag{4}$$

being $w(x)$ the vertical deflection of the rail, $\theta(x)$ the rotation of the rail, ρ the rail density, A the area of the cross-section, $A_s = \kappa A$ the reduced shear area, G the shear modulus, E the Young's modulus, I is the second moment of area of the cross section, and κ the Timoshenko shear coefficient. In this study, the rail type UIC 60 is used, with a value $\kappa = 0.4$. Primes represent spatial derivatives (e.g. $w' = \mathrm{d}w/\mathrm{d}x$) and dots time drivatives (e.g.$\ddot{\theta} = \mathrm{d}^2\theta/\mathrm{d}t^2$)

The sleepers tie the two rails together providing their monolithic actions on the track. These are positioned between the rails and the ballast or slab and the sleepers are modeled with mass point element.

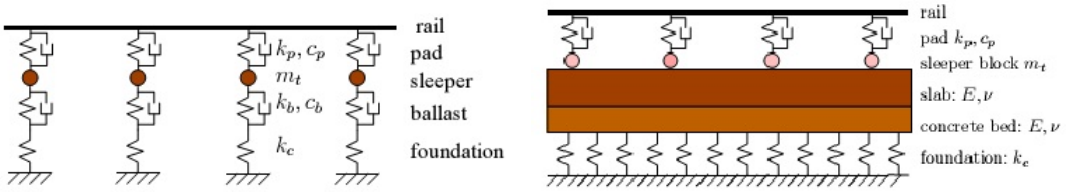

(a) Ballast track model

(b) Slab track model

Figure 6: Track model

For the ballast track model, the subballast is not considered, the ballast is considered as a piramid trunk in order to calculate the effective stiffness and the damping coefficients. In this model, the ballast is considered a vertical spring with damping and the continuity of the ballast in the longitudinal direction is not considered. The foundation is point supports.

We have monitored many point of infrastructure to get the results more adequate about the vertical dynamic response on the infrastructure: the contact point between the vehicle and the rail to obtain the vertical acceleration and then to obtain wheel rail contact force, 13 points of railpad supports to measure forces transmitted to the infrastructure.

3 Generation of track irregularities by random process

Track irregularities play an important role in the dynamic response due to passing trains. Generally, the track irregularities can be approximately represented as stationary and ergodic random processes in space due to its random nature, where the rail quality information is characterized by the power spectral density (PSD) functions [14]. The PSD function depends on the route frequency (Ω), which is expressed as in the equation (5).

$$\Omega = \frac{2\pi}{L}\,, \tag{5}$$

where L is the length of the irregularities (or wave length).

The analytical expression of the PSD functions for the generation of track irregularities have been proposed by many organizations and institutes for application in practice, such as CSD, CKD, SZD of the Czech Republic, SNCF of France, FRA of the USA [14]. Thus, the different PSD functions are used depending on the characteristics of the rail used in each country. In this study, the PSD function proposed by H. Claus and W. Schiehlen [15] is used. The analytical PSD function are published as $one - sided$ density functions:

$$\Phi_V(\Omega) = A\frac{\Omega_c^2}{(\Omega_r^2 + \Omega^2)(\Omega_c^2 + \Omega^2)} \tag{6}$$

where $\Phi_V(\Omega)$ stand for the vertical profile density. The values of the constant factors Ω_r, Ω_c are:

$$\Omega_r = 0.0206\,(\text{rad/m}) \tag{7}$$

$$\Omega_c = 0.8246\,(\text{rad/m}) \tag{8}$$

The scalar factor A is chosen so as to obtain a mean square of the irregularities in the range of 1 to 1.5 mm

$$A = 3.65 \cdot 10^{-6}\,(\text{rad m}) \tag{9}$$

With the PSD function obtained by the analytical expression, the vertical track irregularities can be produced by the inverse Fourier transform shown as in the following equation (10):

$$r(x) = \sqrt{2}\sum_{n=0}^{N-1} A_n cos(\Omega_n x + \varphi_n) \tag{10}$$

considering the spectral density of N discrete frequencies Ω_n. The independent random phase angles φ_n (n=0,1,.....,N-1) are uniformly distributed in the range [0,2π]. The frequencies are set to

$$\Omega_n = n\Delta\Omega = n\frac{\Omega_{max} - \Omega_{min}}{N} \tag{11}$$

where the $\Omega_{max}, \Omega_{min}$ are the lower and upper limits in which the PSD function is defined. The coefficients A_n are used as in [15]:

$$A_o = 0, \tag{12}$$

$$A_1 = \sqrt{(\frac{1}{2\pi}\Phi(\Delta\Omega) + \frac{4}{12\pi}\Phi(0))\Delta\Omega} \tag{13}$$

$$A_2 = \sqrt{(\frac{1}{2\pi}\Phi(2\Delta\Omega) + \frac{1}{12\pi}\Phi(0))\Delta\Omega} \tag{14}$$

$$A_n = \sqrt{(\frac{1}{2\pi}\Phi(\Omega_n)\Delta\Omega} \tag{15}$$

In this study, the vertical irregularities rail were developed according to the equation (10) with two cases of wavelength range which are defined in prEN 13848-5 [16] (D1 is wavelength in range [3m,25m], D2 is very short wavelength in range [0.05 m, 3m])

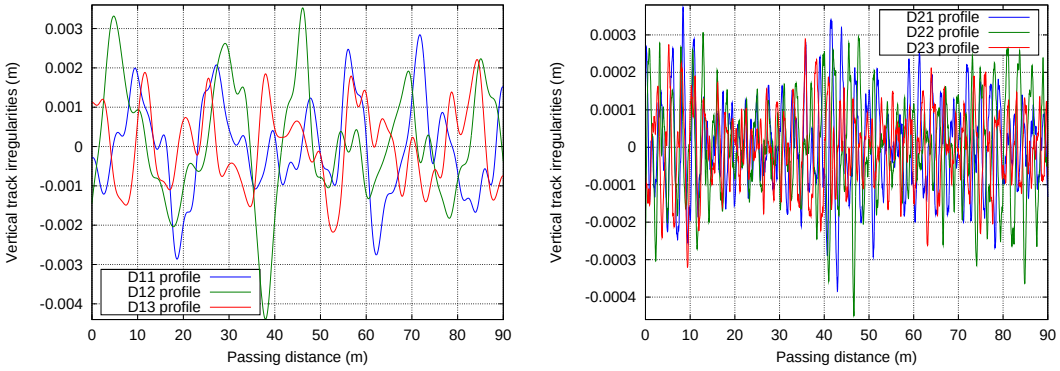

(a) D1 wavelength (b) D2 very short wavelength

Figure 7: Vertical track irregularities with respect to passing distance

Figure 7 shows the vertical irregularities used in this study for two cases of wavelength range.

To verify the correct generation of track irregularities, the reverse process is taken place, that is obtaining the PSD as the Fourier transform of the autocorrelation function of track irregularities generated according to the Eq. (10) and compare with the curve of the PSD used analytical in Eq. (5). Figure 8 shows some power spectral densities of the generated irregularities profiles and the analytical ones.

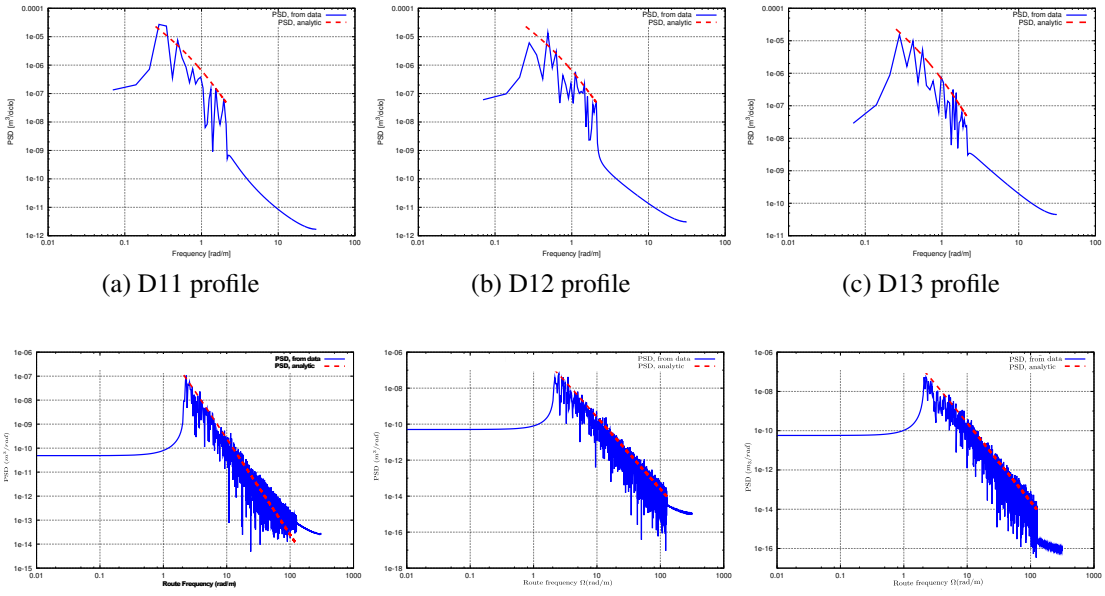

(a) D11 profile (b) D12 profile (c) D13 profile

(d) D21 profile (e) D22 profile (f) D23 profile

Figure 8: Power spectral densities

4 Cases studied and aplications

4.1 Ballast track

The classical ballast track basically consists of a platform made up of the rails and sleepers which are supported on ballast. The ballast rests on a sub-ballast layer which forms the transition layer to the platform (see Fig 9). The ballast track was modeled using 2D finite elements, the track length studied in the models is 90.0 m, modeling only a single rail. The different components of track modeled were the platform through a coefficient of ballast, the sleepers, the rail pads and the rail.
The model parameters are listed in Table 4.

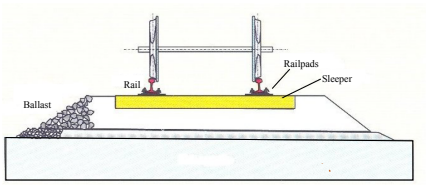

Figure 9: The scheme of cross section of ballast track

Dimensions	
Model length	90.0 m
Ballast thickness	40 cm
Separation pads	0.60 m
Properties	
Rail	UIC60
Pads stiffness (k_p)	100 kN/mm
Damping pads (c_p)	0.015 kN s/mm
Ballast stiffness (k_b)	100 kN/mm
Damping ballast (c_b)	0.0123 kN s/mm
Mass of half sleeper ($m_t/2$)	160 kg
Point foundation stiffness (k_c)	80 kN/mm

Table 4: Model parameters of ballast track

4.2 Rheda track

The Rheda system has been under continuous development since its first application in 1970. The Rheda 2000 Slab Track System has resulted from the ongoing development of the well known German Rheda system.The slab track Rheda 2000 scheme considered is shown in figure 11. The slab track Rheda 2000 was modeled using 2D

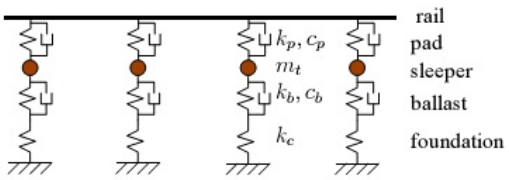

Figure 10: Detail of the finite element mesh ballast track

finite elements. The track length studied in this case is 97.5 m, considering only a single rail. The different components of track modeled were the platform through a coefficient of ballast, the concrete slab, the sleepers, the rail pads and the rail.
The model parameters are listed in Table 5.

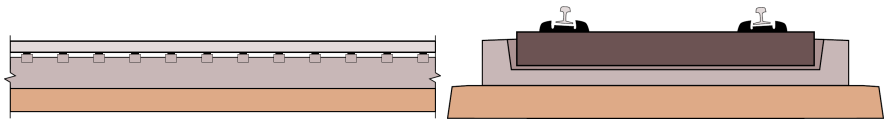

Figure 11: The scheme of longitudinal and cross section of Rheda 2000 track

Dimensions	
Model length	97.5 m
Slab thickness	24 cm
Separation pads	0.65 m
Properties	
Rail	UIC60
Elastic modulus of concrete (E_h)	34 GPa
Pads stiffness (k_p)	40 kN/mm
Damping pads (c_p)	0.008 kN s/mm
Ballast module platform (k_c)	80 kN/mm
Mass of half sleeper ($m_t/2$)	69 kg

Table 5: Model parameters of slab track Rheda 2000

4.3 Aftrav track

The slab track Aftrav scheme considered for modeling is shown in figure 13. The slab track Aftrav was modeled using 2D finite elements. The track length studied in this case is 93.55 m, considering only a single rail. The different components of track modeled were the platform through a coefficient of ballast, the concrete slab, the sleepers, the rail pads and the rail.
The model parameters are listed in Table 6.

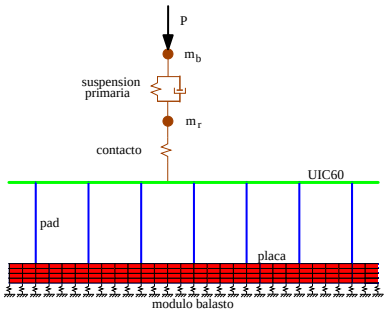

Figure 12: Detail of the finite element mesh slab track Rheda 2000

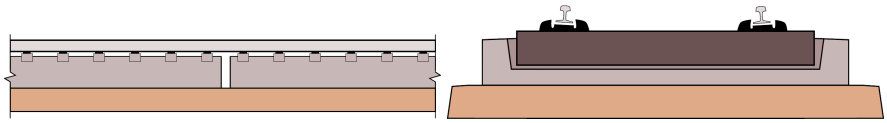

Figure 13: The scheme of longitudinal and cross section of Aftrav track

Dimensions	
Model length	93.55 m
Slab thickness	20 cm
Separation pads	0.65 m
Properties	
Rail	UIC60
Elastic modulus of concrete (E_h)	27 GPa
Pads stiffness (k_p)	40 kN/mm
Damping pads (c_p)	0.008 kN s/mm
Ballast module platform (K_c)	80 kN/mm
Mass of half sleeper ($m_t/2$)	69 kg

Table 6: Model parameters of slab track Aftrav

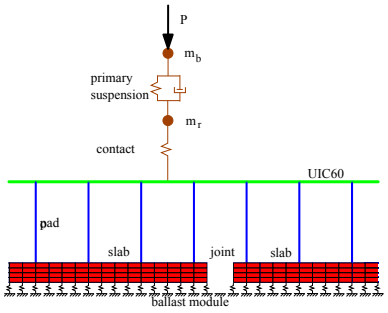

Figure 14: Detail of the finite element mesh slab track Aftrav

4.4 Dynamic responses of vehicle and track

The results obtained of the computations are shown in Figure 15- 20. These include the wheel-rail contact force, forces transmitted to the bogie by the primary suspension, and forces transmitted to the infrastructure (sleeper or slab) by the railpads, and the envelope of the results.
Figure 15 shows the wheel-rail contact force in the ballast model when the vehicle travels along the track with distinct vertical random irregularities at 360 km/h and compare with the static force. The dynamic amplification factor at this velocity is 1.337 for the D11 profile, and is 1.398 for the D21 profile.
Figure 16 shows the forces transmitted to the railpads in the Rheda model when the vehicle travels along the track with distinct vertical random irregularities at 300 km/h.
Figure 17 shows the envelope of the results of the dynamic amplification factor of contact force in distinct profile of Ballast model and Rheda model with the D1 profile. With increase of the train speed, the dynamic amplification factor increases too. The maximum factor is obtained at the velocity 360 km/h in both profile.
Figure 18 shows the envelope of the results of the dynamic amplification factor of forces transmitted to railpads in D1 profile of Ballast model and Rheda model.
Figure 19 shows the envelope of the results of the forces transmitted to the bogie by the primary suspension in distinct profile of Ballast model. The maximum force value is obtained at the velocity 320 km/h in D1 profile.
Figure 20 shows the envelope of the results of the dynamic amplification factor of forces transmitted to the bogie by the primary suspension in D1 profile of Rheda model. This shows that increasing speed is not always increase the forces corresponding. The maximum factor value is obtained at the velocity 280 km/h in D1 profile.
In view of the graphics, we derive the following results:

- The vertical interaction forces between the wheel and the rail, forces transmitted to the bogie by the suspension and forces transmitted to the infrastructure by the railpads are very sensitive both to irregularity of the track and train speeds.

- The dynamic responses are very similar for all track models when the random track irregularities are used with the wavelengths between the normal range [3m;25m] (see table. 7). But when using the irregularity of track with a very short wavelengths in the range [0.05 m, 3m], the dynamic responses are very dispersed for each track model, the Rheda track and the Aftrav track have better behavior of others (see table. 7).

- The results of the Aftrav model and the Rheda model are similar, so in this paper we only present the graphic results of the Rheda model.

Model type	Cont. D1	Cont. D2	Pads.D1	Pads. D2
Ballast	1.33	2.80	1.25	2.40
Rheda 2000	1.32	1.65	1.24	1.55
Aftrav	1.33	1.71	1.29	1.58

Table 7: Maximum dynamic amplification factor

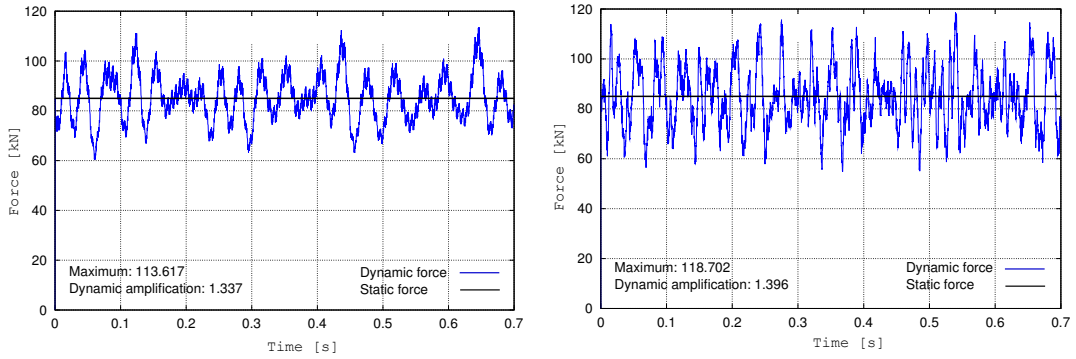

(a) D11 profile (b) D21 profile

Figure 15: Wheel-rail contact force in distinct profile with vehicle speed v=360km/h of ballast model.

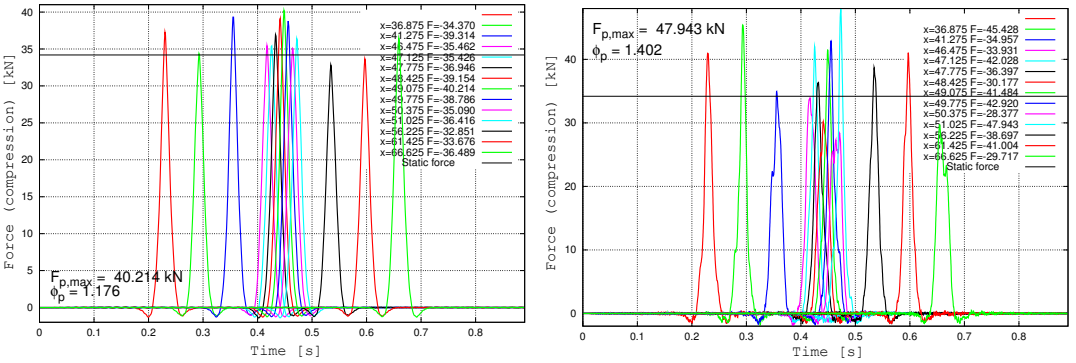

(a) D11 profile (b) D21 profile

Figure 16: Forces transmitted to railpads in distinct profile with vehicle speed v=300km/h of Rheda model.

5 Conclusion

In this study, a 2D finite element model for the analysis of high-speed railway interaction was proposed, in which various improved finite elements were adopted to model the structural constituents of railway.

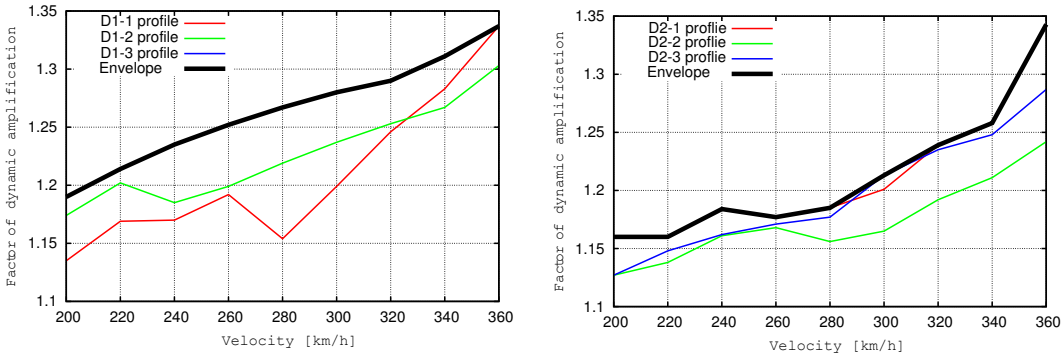

(a) Ballast track (b) Rheda track

Figure 17: Factor of dynamic amplification of contact force in D1 profile.

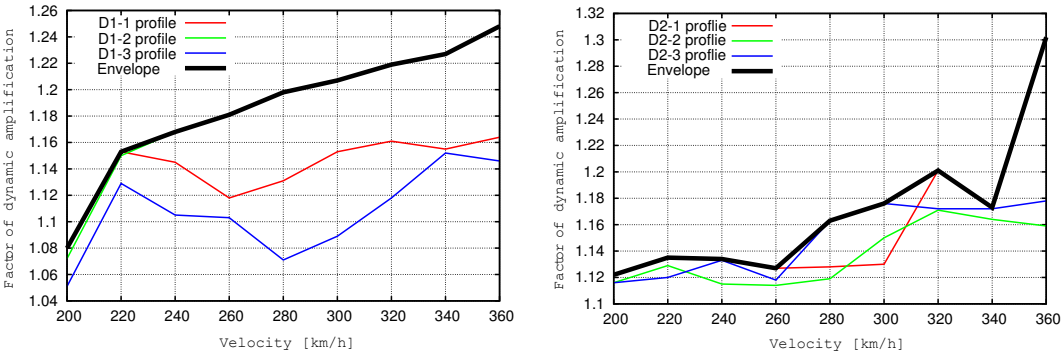

(a) Ballast track (b) Rheda track

Figure 18: Factor of dynamic amplification of force transmitted to railpads in D1 profile.

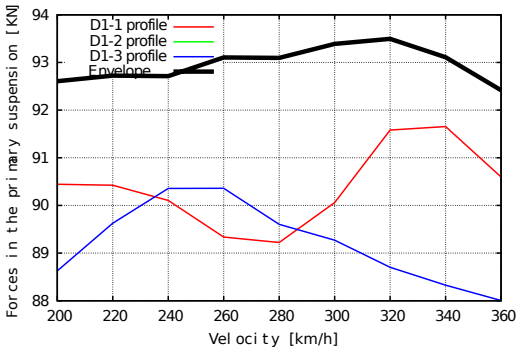

Figure 19: Force transmitted to the bogie by the primary suspension in D1 profile of Ballast model.

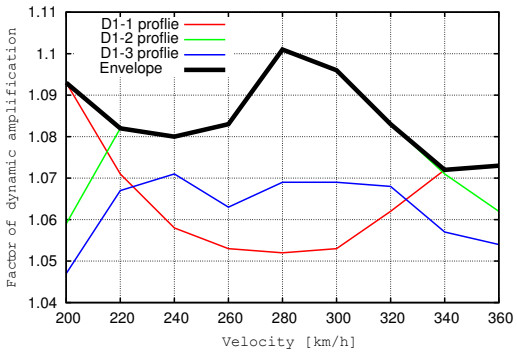

Figure 20: Dynamic amplification factor of forces transmitted to the bogie by the primary suspension in D1 profile of Rheda model.

The track vertical profile irregularity is considered as stationary ergodic Gaussian random processes, which is included in calculating the contact forces with the penalty method [17]. The dynamic responses are very sensitive both to the track irregularities and the vehicle speed.

The model reported in this paper is capable of predicting the dynamic responses of both the vehicle and the rail track components. The model is also capable of examining the influence of the properties of the rail track and the wagon components on the contact force and other dynamic responses of the rail track and vehicle system.

The traditional ballast track has the similar dynamic behavior to other types of track when the track has adequate quality.

Acknowledgements

The authors acknowledge the financial support of Ministerio de Fomento of Spain - CEDEX to the project “Estudio del comportamiento a medio y largo plazo de las estructuras ferroviarias de balasto y placa” (Ref. PT-2006-024-19CCPM-Proyecto de investigacion del Plan Nacional)

References

[1] M. Melis, “Embankments and Ballast in High Speed Rail. Fourth part: High-speed railway alignments in Spain. Certain alternatives”, *Revista de Obras Pblicas*, 3476: 41–66, april 2007.

[2] S. Timoshenko, D. Young, *Vibration problems in engineering*, Van Nostrand, NY, third edition, 1995.

[3] L. Fryba, *Vibration of solids and structures under moving loads*, Thomas Telford, third edition, 1999.

[4] Y. Sun, M. Dhanasekar, "A dyanmic model for the interaction of the rail track and wagon system", *International Journal of Solids and Structures*, 39: 1337–1359, 2002.

[5] C. Esveld, *Modern Railway Track*, MRT Productions, 2001.

[6] K. Vijay, V. Rao, *Dynamics of Railway Vehicle Systems*, Academic Press, Canada, 1984.

[7] X. Lei, N. Noda, "Analyses of dynamic response of vehicle and track coupling system with random irregularity of track vertical profile", *J. Sound Vib.*, 258: 147–165, (2002).

[8] Y. Yang, J. Yau, Y. Wu, *Vehicle-Bridge Interaction Dynamics with applications to high-speed railways*, World Scientific Publishing Co. Pte. Ltd., 2004.

[9] K. Popp, I. Kaiser, H. Kruse, "System dynamics of railway vehicles and track", *Archive of Applied Mechanics*, 72(11-12/June), (2003).

[10] M. Song, H. Noh, C. Choi, "A new three-dimentional finite element analysis model of high speed train-bridge interactions", *Engineering Structures*, 25: 1611–1626, (2003).

[11] Q. Zhang, A. Vrouwenvelder, J. Wardenier, "System dynamics of railway vehicles and track", *Archive of Applied Mechanics*, 72(11-12/June), (2003).

[12] N. Dinh, K. Kim, P. Warnitchai, "Simulation produce for vehicle-subtructure dynamic interactions and wheel movements using linearized wheel-rail interfaces", *Finite Elements in Analysis and Design*, 45: 341–356, (2009).

[13] K. Johnson, *Contact Mechanics*, Cambridge University Press, UK, 1985.

[14] L. Fryba, *Dynamics of railways bridges*, Thomas Telford, 1996.

[15] H. Clauss, W. Schiehlen, "Modeling and Simulation of railways bogie structural vibrations", *Vehicle System Dynamics*, 29(S1): 538–552, 1998.

[16] C.. prEN 13848-5, "Railway applications, Track, Track geometry, Part 5: Geometric quality assessment.", *European Committee for Standardization (CEN).*

[17] R. Taylor, *FEAP-A Finite Element Analysis Program. Version 7.5 User Manual.*, 2004.